Published in final edited form as:

Cancer Res. 2021 March 01; 81(5): 1240–1251. doi:10.1158/0008-5472.CAN-20-0118.

Oncogenic N-Ras Mitigates Oxidative Stress–Induced Apoptosis of Hematopoietic Stem Cells

Gina M. Ney[1], **Kevin B. Yang**[2], **Victor Ng**[2], **Lu Liu**[2], **Meiling Zhao**[2], **Wun Kuk**[2], **Lila Alaka**[2], **Leilani Sampang**[2], **Adam Ross**[2], **Morgan A. Jones**[2], **Xi Jin**[2], **Laura M. McKay**[1], **Hadie Evarts**[2], **Qing Li**[2,3]

[1]Department of Pediatrics, University of Michigan, Ann Arbor, Michigan.

[2]Department of Internal Medicine, University of Michigan, Ann Arbor, Michigan.

[3]Department of Cell and Developmental Biology, University of Michigan, Ann Arbor, Michigan.

Abstract

Leukemic relapse is believed to be driven by transformed hematopoietic stem cells (HSC) that harbor oncogenic mutations or have lost tumor suppressor function. Recent comprehensive sequencing studies have shown that mutations predicted to activate Ras signaling are highly prevalent in hematologic malignancies and, notably, in refractory and relapsed cases. To better understand what drives this clinical phenomenon, we expressed oncogenic *Nras*^{G12D} within the hematopoietic system in mice and interrogated its effects on HSC survival. N-Ras^{G12D} conferred a survival benefit to HSCs and progenitors following metabolic and genotoxic stress. This effect was limited to HSCs and early progenitors and was independent of autophagy and cell proliferation. N-Ras^{G12D}–mediated HSC survival was not affected by inhibition of canonical Ras effectors such as MEK and PI3K. However, inhibition of the noncanonical Ras effector pathway protein kinase C (PKC) ameliorated the protective effects of N-Ras^{G12D}. Mechanistically, N-Ras^{G12D} lowered levels of reactive oxygen species (ROS), which correlated with reduced mitochondrial membrane potential and ATP levels. Inhibition of PKC restored the levels of ROS to that of control HSCs and abrogated the protective effects granted by N-Ras^{G12D}. Thus, N-Ras^{G12D} activation within HSCs

Corresponding Author: Qing Li, University of Michigan–Ann Arbor, 109 Zina Pitcher Place, BSRB 152, Ann Arbor, MI 48109. lqing@med.umich.edu.

G.M. Ney, K.B. Yang, and V. Ng contributed equally to this study.

Authors' Contributions

G.M. Ney: Conceptualization, data curation, formal analysis, investigation, methodology, writing–original draft. **K.B. Yang:** Conceptualization, data curation, formal analysis, investigation, methodology, writing–original draft. **V. Ng:** Conceptualization, data curation, formal analysis, investigation, methodology, writing–original draft. **L. Liu:** Data curation, formal analysis, investigation, methodology. **M. Zhao:** Data curation, formal analysis, validation. **W. Kuk:** Data curation, formal analysis, investigation. **L. Alaka:** Data curation, formal analysis, investigation. **L. Sampang:** Data curation, formal analysis, investigation. **A. Ross:** Data curation, formal analysis, investigation. **M.A. Jones:** Data curation, formal analysis, validation, investigation. **X. Jin:** Data curation, formal analysis, investigation. **L.M. McKay:** Conceptualization, resources, data curation, formal analysis, supervision, funding acquisition, validation, investigation, visualization, methodology, writing–original draft, project administration, writing–review and editing. **H. Evarts:** Data curation, formal analysis. **Q. Li:** Conceptualization, resources, data curation, formal analysis, supervision, funding acquisition, validation, investigation, visualization, methodology, writing–original draft, project administration, writing–review and editing.

Supplementary data for this article are available at Cancer Research Online (http://cancerres.aacrjournals.org/).

Authors' Disclosures

G.M. Ney reports grants from NIH, St. Baldrick's Foundation, and Hyundai Hope on Wheels during the conduct of the study, as well as patents 8,324,258 and 8,497,307 issued, licensed, and with royalties paid from Lycera Inc. No disclosures were reported by the other authors.

promotes cell survival through the mitigation of ROS, and targeting this mechanism may represent a viable strategy to induce apoptosis during malignant transformation of HSCs.

Introduction

RAS and Ras-activating mutations have been identified as initiating genetic lesions, frequent molecular events, and prognostic markers across a range of cancers (1, 2). This includes pancreatic, lung, colon, and rhabdomyosarcoma in solid tumors, and acute myeloid and lymphoblastic leukemia and juvenile myelomonocytic leukemia in hematologic malignancies. In addition, with the wide availability of clinical sequencing, mutations predictive of hyperactive Ras signaling have also now been correlated with disease relapse and treatment refractoriness (3–9). Thus, understanding how dysregulated Ras signaling contributes to each of these outcomes is of critical importance to improve our understanding of disease development and treatment algorithms to better serve patients with cancer.

Leukemogenesis is a process during which hematopoietic stem cells and progenitors (HSC/P) are transformed into leukemic stem cells (LSC) following mutations that activate oncogenes or inactivate tumor suppressor genes (10). Importantly, LSCs have been shown to escape extensive chemo- and/or radiotherapy and persist even after patients achieve clinical remission, thus harboring a focus for disease relapse (11–13). These studies suggest that the successful treatment of leukemia depends on better defining and eliminating LSCs.

Despite accumulating evidence that *RAS* mutations contribute to treatment resistance in leukemia, little is known about the potential role of oncogenic Ras signaling in the survival of HSC/Ps and how it may contribute to this process. Previously, we and others reported that mice harboring an oncogenic *Nras* mutation, *G12D*, expressed from its endogenous locus develop an indolent disease with features reminiscent of chronic and juvenile myelomonocytic leukemia (CMML/JMML; refs. 14, 15). Strikingly, when additional genetic mutations were introduced in this model, oncogenic N-Ras collaborated with these lesions to reproducibly induce acute myeloid leukemia (AML; ref. 14). We subsequently reported that oncogenic N-Ras^{G12D} exerts profound effects on HSCs, resulting in their dysregulation to promote HSC self-renewal and clonal expansion (16). However, whether oncogenic N-Ras confers a survival phenotype to HSCs to promote these processes is not known.

To address this question, we utilized our previously established *Nras*^{G12D} model and interrogated the effects of hyperactive N-Ras on HSC survival. We report that hyperactive N-Ras signaling confers a survival advantage to HSC/Ps. Specifically, *Nras*^{G12D} HSCs and early progenitors exhibit resistance to metabolic and genotoxic stress induced by radiation and chemotherapy, and this effect was mediated by decreased reactive oxygen species (ROS) and lower mitochondrial activity. Furthermore, this effect was independent of the canonical Ras pathways MEK/ERK and PI3K/AKT/mTOR but was instead mediated via enhanced protein kinase C (PKC) activity. Ultimately, targeting noncanonical Ras effector pathways and/or destabilizing redox stress may represent novel therapeutic strategies to overcome treatment resistance in Ras-mutated hematologic malignancies.

Materials and Methods

Animals

All mice were housed in the Unit for Laboratory Animal Medicine at the University of Michigan, and protocols were approved by the University of Michigan Committee on the Use and Care of Animals (PRO00007786). Conditional *Nras*^{G12D} knockin mice (14), *Stat5ab* knockout mice (16), and transgenic *Col1A1-H2B-GFP; Rosa26-M2-rtTA* mice (17) were described previously. All animals were maintained on a C57/BL6 background. Littermates or age- and gender-matched mutant and control mice (6–10 weeks of age) were used for all experiments. To activate *Nras*^{G12D}, the *Mx1-cre*$^{+}$*; Nras*$^{LSL\text{-}G12D/+}$ mice received intraperitoneal injections of poly (I:C; GE Healthcare Life Sciences 27-4732-01) at a dose of 0.5 μg/g body mass every other day for three doses 2 weeks before analysis. Doxycycline was added to the water at a concentration of 0.2% (m/v) along with 1% sucrose. No difference of phenotype was observed between male and female mice.

Antibodies

PKC antibodies were used as follows: PKCδ (Santa Cruz Biotechnology; C-20; catalog no. SC-937) was used at dilution of 1:500, PKCδ (Cell Signaling Technology; catalog no. 2058S) was used at dilution of 1:1,000, PKCε (Santa Cruz Biotechnology; C-15; catalog no. SC-214) was used at dilution of 1:1,000, PKCθ (Santa Cruz Biotechnology, and C-18; catalog no. SC-212) was used at dilution of 1:1,000, PKCη (Santa Cruz Biotechnology; 31; catalog no. SC136036) used at dilution of 1:1,000. β-Actin (8H10D10) was purchased from Cell Signaling Technology (3700S).

Statistical analysis

Group data represent mean ± SD. *N* represents the number of biological replicates and is indicated in figure legends. Statistical analysis for each experiment is specifically described in the corresponding figure legend. GraphPad Prism software was used unless otherwise indicated. A minimum of three independent experiments were performed to verify reproducibility. Two-tailed Student *t* tests were used to assess statistical significance for two group comparisons and ANOVA tests were performed for more than two groups.

Flow cytometry and isolation of HSCs

Bone marrow cells were harvested and cell populations were isolated as described previously (16). Briefly, the bilateral hips, legs, and spine were placed in HBSS containing 3% filtered calf serum and crushed with a mortar and pestle. Staining was completed in two steps: first using HSC SLAM cocktail (all BD Biosciences), after which, c-kit enrichment was performed using MACS anti-APC or anti-biotin beads and enriched on LS magnetic column (Miltenyi). Annexin V staining was performed according to commercially provided protocols (BD Biosciences; 556547). ROS staining was performed with CellROX reagent according to manufacturer's instructions and used at a final concentration of 5 μmol/L (Thermo Fisher Scientific; C10422). Tetra-methylrhodamine methyl ester (TMRM) was used according to manufacturer's instructions at a final concentration of 0.5 μmol/L (Thermo Fisher Scientific; T668 and M7514). HSC sorting was completed using DIVA

software on a BDAria cell sorter or Sony SA400 and analysis completed with BD LSR Fortessa using FlowJo software.

In vitro cell culture

For cytokine starvation assays, equal numbers of HSCs (typically 300–1,000) were sorted into 100 μL of SF-O3 medium (Iwai North America Inc.) supplemented with 1% bovine serum albumin, with or without cytokines [stem cell factor (SCF) and thrombopoietin (TPO); 100 ng/mL each; Peprotech 250–03 and 315–14] and cultured for 18 hours. Cleaved caspase-3/7 assays were then performed according to manufacturer's protocol (Promega G8090).

Ex vivo analysis

ATP levels were measured immediately after sorting 400 HSCs into SF-O3 media with cytokines, according to manufacturer's instructions using Cell-Titer Glo Assay (Promega G7570). Total and oxidized glutathione levels were measured in 1,000 sorted CD48-$Lin^{-}Sca\text{-}1^{+}c\text{-}Kit^{+}$ (LSK) using the GSH/GSSG-Glo Assay by Promega according to instructions. To perform colony forming assays, 200 to 400 FACS-sorted HSCs were plated in duplicates into 12-well plates containing Methocult 3434 medium (Stem Cell Technologies; 3434), cultured for 7 days and counted.

mtDNA

A total of 40,000 LSKs were sorted into DirectPCR (Viagen Biotech 102-T) with proteinase K and heated overnight at 55°C. DNA was isolated following ethanol purification using standard methods. Primer sequences are as followed: ND-1: CTAGCAGAAACAAACCGGGC (forward) CCGGCTGCGTATTCTACGTT (reverse); actin: CGGCTTGCGGGTGTTAAAAG (forward) CGTGATCGTAGCGTCTGGTT (reverse).

Other

For qRT-PCR, primer sequences were as followed: PKCα: CGCTCCACACTGAATCCTC (forward) CGGCATCTTCATTAGCTCT (reverse); PKCβ: CCGCGACCTGAAACTTGACA (forward) CTCCAAATGCCCACCAGTCCA (reverse); PKCδ: TGCAAGAAGAACAACGGCAA (forward) CTGTTTAATGGCTCCACGAC (reverse); PKCε: TGACCAAGAACCCGCACAA (forward) TATTGGCTCTTCCCGCGTA (reverse); PKCθ: ATCTTTCCAGAGCCACGTTT (forward) TGTCTTCGCATCTCCTAGCAT (reverse).

Results

Oncogenic N-Ras^{G12D} protects HSCs from apoptosis

We previously reported that HSCs expressing a single copy of oncogenic $Nras^{G12D}$ durably out-compete their wild-type counterparts through increased self-renewal and competitiveness (16). Given that tight regulation of apoptosis has been shown to provide a competitive advantage to HSCs (18), we asked whether this mechanism could be

relevant after introduction of oncogenic N-Ras^{G12D}. To address this question, we generated *Mx1-Cre*$^{+}$*; Nras*$^{LSL\text{-}G12D/+}$ mice (referred to hereafter as *Nras*^{G12D} or *Nras* mutant mice) using a previously described *Nras*^{G12D} allele in which the *G12D* mutation was expressed endogenously from the *Nras* locus downstream of a floxed "STOP" cassette that represses transcription (14, 16). To delete the "STOP" cassette and activate the mutant *G12D* allele in hematopoietic tissues, we administered three doses of poly-inosine:poly-cytosine (pIpC) over a 5-day period (at a dose of 0.5 μg/g body mass) to 6- to 10-week-old *Nras*^{G12D} mice. The mice were then analyzed a minimum of 2 weeks after pIpC treatment and paired with gender- and age-matched controls that lacked a *Cre* allele (*Nras*$^{LSL\text{-}G12D/+}$ only mice).

To assess whether N-Ras^{G12D} protects HSCs from apoptosis, we isolated SLAM HSCs (Lineage^{-}c-Kit^{+}Sca-1^{+}CD48^{-}CD150^{+}; Supplementary Fig. S1; ref. 19) from control and *Nras*^{G12D} mice and subjected them to either cytokine starvation for 18 hours or 300 cGy of ionizing radiation (IR), which induces apoptosis via metabolic, oxidative, and genotoxic stress (20–22). Apoptotic cells were then measured using both Annexin V positivity by flow cytometry and cleaved caspase-3/7 level. HSCs cultured under growth conditions in the presence of cytokines (SCF and TPO; both at 100 ng/mL) showed no difference in apoptosis between *Nras*^{G12D} and control HSCs. However, *Nras*^{G12D} HSCs demonstrated reduced frequency of Annexin V-positive cells (Fig. 1A and B) and lower levels of cleaved caspase-3/7 (Fig. 1C) in the absence of cytokines. To assess if N-Ras^{G12D} afforded protection following clinically relevant therapies, we subjected *Nras*^{G12D} HSCs to γ-irradiation (3 Gy; Fig. 1D), as this has been shown to induce apoptosis in HSCs (20). Similar to conditions of cytokine starvation, *Nras*^{G12D} HSCs were more resistant to γ-irradiation–induced apoptosis, as demonstrated by Annexin V positivity and caspase 3/7 activation (Fig. 1E and F). Thus, N-ras^{G12D} promoted HSC survival *in vitro* following metabolic and genotoxic stress.

Given that HSCs reside in a protective bone marrow niche, we next validated the protective effects of N-Ras^{G12D} *in vivo*. *Nras*^{G12D} mice and controls were treated with a sublethal dose (3 Gy) of γ-irradiation. Twenty-four hours following exposure, whole bone marrow (WBM) was harvested and apoptosis measured following cell surface marker staining (Fig. 2A; Supplementary Fig. S2). Both *Nras*^{G12D} SLAM HSCs and LSK hematopoietic progenitor cells were protected from apoptosis as indicated by reduced frequencies of Annexin V^{+} cells (Fig. 2B and C). Importantly, this protective effect of N-ras^{G12D} was restricted to hematopoietic stem and progenitor cells but not observed in differentiated lineage-committed cells (Fig. 2C). These data demonstrate that N-Ras^{G12D} exerts a prosurvival phenotype to HSCs and early progenitors *in vivo* and could therefore allow transformed HSC/Ps to persist following intensive therapeutic regimens. Next, to understand if HSC function is retained following *in vivo* radiation, 400 HSCs were FACS sorted from sublethally irradiated (3 Gy) *Nras*^{G12D} and control mice and plated in methocellulose media with cytokines (SCF and TPO; both at 100 ng/mL). After 7 days of culture, *Nras* mutant HSCs formed significantly more colonies than control HSCs (Fig. 2D), suggesting hyperactive N-Ras^{G12D} preserves HSC function after exposure to genotoxic agents. Furthermore, to test the impact of radiation on HSC function *in vivo*, we administered a dose of 3 Gy γ-radiation to CD45.2 control and *Nras* mutant mice and 24 hours later, transplanted whole bone marrow from these mice to lethally irradiated CD45.1 recipient mice, together

with wild-type CD45.1 radioprotector cells (at a ratio of 10:1; Fig. 2E). Peripheral blood chimerism was then measured up to 24 weeks posttransplantation (Fig. 2F; Supplementary Fig. S3). As reported previously (16), unirradiated *Nras* mutant marrow showed enhanced reconstitution relative to control (Fig. 2F). Following radiation, *Nras* mutant HSCs preserved the enhanced reconstitution, and showed a trend of further increase of reconstitution relative to irradiated wild-type HSCs, suggesting that despite cellular insult, N-Ras^{G12D} bestows a competitive advantage *in vivo* to HSCs.

We then considered additional treatment *in vivo*, and chose to administer four weekly doses of 5-fluorouracil (5-FU; 150 mg/kg/dose), which ablates proliferative cells within the bone marrow and relies on intact HSC function to restore hematopoiesis. Although increased HSC proliferation typically leads to increased sensitivity to 5-FU treatment, despite our previous report that N-ras^{G12D} increases the overall proliferation of the HSC pool (16), we observed prolonged survival in *Nras^{G12D}* mice after 5-FU treatment (Fig. 2G). Although all wild-type control mice became moribund or died by day 20, 50% of *Nras^{G12D}* mice survived by day 30. To understand if N-Ras^{G12D} provides a survival advantage to HSCs after 5-FU, we administered a single dose of 5-FU and monitored peripheral blood cell recovery by myeloid percentage every 3 days. We observed that *Nras* mutant mice had a quicker recovery of peripheral blood myeloid cells (Fig. 2H), suggesting that N-Ras^{G12D} confers a survival advantage under stress.

The prosurvival phenotype of *Nras^{G12D}* HSC is independent of autophagy

Evolving data have shown that autophagy is critical to HSC maintenance, self-renewal, and survival (21, 23, 24), specifically under conditions of HSC stress and during leukemogenesis (25). To test whether induction of autophagy is responsible for the survival phenotype of *Nras^{G12D}* HSCs, we treated HSCs with bafilomycin A (BafA), which inhibits the late phase of autophagy by preventing fusion of autophagosomes with lysosomes, under conditions of cytokine starvation (Supplementary Fig. S4A; refs. 21, 26). Inhibition of autophagy via bafilomycin A did not diminish the resistance of *Nras^{G12D}* HSCs to apoptosis as detected by caspase-3/7 activation (Supplementary Fig. S4B). To confirm these findings, we measured autophagocytic activity by selectively labeling accumulated autophagocytic vacuoles with Cyto-ID. As has been previously shown, control HSCs upregulated autophagy under conditions of cytokine starvation (21), but there was no difference in Cyto-ID levels between *Nras^{G12D}* and control HSCs after cytokine starvation (Supplementary Fig. S4C). Consistent with these findings, microarray analysis of gene expression (GSE45194; ref. 16) demonstrated similar mRNA levels of key autophagy regulators in control and *Nras^{G12D}* HSCs (Supplementary Fig. S4D). Taken together, these data indicate that autophagy is not a significant mediator of enhanced HSC survival induced by oncogenic N-Ras^{G12D}.

PKC signaling mediates protection from apoptosis in *Nras^{G12D}* HSCs

The downstream signaling pathways following Ras activation are well-characterized to promote cell survival and proliferation in many cancers. To identify the potential signaling mediators of N-Ras^{G12D}–induced survival in HSCs, we treated HSCs with a series of compounds that inhibit the canonical downstream pathways of the Ras (2) and exposed HSCs to cytokine starvation (Fig. 3A; Supplementary Table S1). Interestingly,

pharmacologic inhibition of the canonical Ras effectors, MEK (PD0325901), PI3K/AKT (GDC-0941), or mTOR (rapamycin), did not affect the survival benefit of *Nras*^{G12D} HSCs under cytokine starvation (Fig. 3A). We previously found that N-Ras^{G12D} upregulates STAT5 signaling to increase HSC proliferation and self-renewal and that heterozygous knockout of *Stat5ab* abolished these effects (16). We therefore interrogated if the prosurvival phenotype of *Nras* mutant HSCs is dependent on STAT5 signaling by generating *Mx1-cre*$^{+}$; *Nras*$^{LSL\text{-}G12D/+}$; *Stat5a*/*b*$^{fl/+}$ mice. We then injected the mice with pIpC (0.5 μg/g body mass every other day for six doses) and 2 weeks after pIpC, purified SLAM HSCs and measured apoptosis by caspase-3/7 activation after cytokine starvation. We found that heterozygous knockout of *Stat5ab* had minimal effects on survival in control or *Nras*^{G12D} HSCs following cytokine starvation (Supplementary Fig. S4E). Together, these data suggest that STAT5 signaling is important for HSC proliferation but not survival of *Nras*^{G12D} HSCs under stress conditions.

To further dissect downstream signaling, we considered noncanonical Ras effectors and, specifically, those that have been reported to play a role in cell survival. Of these downstream pathways, PKC isoenzymes have been reported to modulate apoptotic signaling (27). Given this, we asked if PKC signaling could contribute to the observed survival advantage in *Nras*^{G12D} HSCs. There are at least 10 known PKC isoforms, which are grouped as classical PKCs (cPKC): PKCα, PKCβI, PKCβII, PKCγ; novel PKCs (nPKC): PKCδ, PKCε, PKCη, PKCθ; and atypical PKCs (aPKC): PKCζ, PKCι. PKCs (cPKC): PKCa, PKCbI, 328 PKCbII, PKCg; novel PKCs (nPKC): PKCd, PKCe, PKCh, PKCq; 329 and atypical PKCs (aPKC): PKCz, PKCi. Each group has distinct intracellular functions and inhibition of many have been interrogated as a therapeutic strategy in cancer, inflammatory diseases, and cardiac injury (27, 28). We therefore chose to administer a series of PKC inhibitors that exhibit selectivity for the various isoforms (Supplementary Table S2). We initiated these studies using two pan-PKC inhibitors, Bisindolylmaleimide I (BIS) and Sotrastaurin (AEB), and found that treatment with these inhibitors under cytokine starvation dramatically abolished the prosurvival phenotype observed in *Nras*^{G12D} HSCs (Fig. 3B and C). We next chose inhibitors selective for cPKC isoforms, LY 333531 (LY33) and GO6976 (GO69), and found that they each had no effect on the survival advantage of *Nras*^{G12D} HSCs, thus eliminating a significant role of the classic PKC isoforms in the antiapoptotic phenotype of *Nras*^{G12D} HSCs (Fig. 3B).

To further test which PKC isoform may induce the observed findings in *Nras*^{G12D} HSCs, we measured expression of several PKC isoforms in control and *Nras*^{G12D} HSCs by real-time PCR. However, we did not observe increased mRNA expression of any PKC isoform in *Nras*^{G12D} HSCs compared with control HSCs (Fig. 3D). Next, we questioned if PKC protein expression could be altered by N-Ras^{G12D}. Notably, both novel and classic PKC isoforms possess a common C2 domain that is activated under stress and could therefore participate in apoptosis (29, 30). Given that inhibition of classic PKC isoforms demonstrated no functional effect in *Nras*^{G12D} cells, we focused on novel PKC isoforms and examined protein levels by Western blot analysis in control and *Nras*^{G12D} HSC/Ps (LSK) cells. As shown, PKCδ levels were increased in *Nras*^{G12D} compared with control LSKs (Fig. 3E), whereas PKCε and PKCΘ showed comparable expression levels in both. Of note, we did not detect a signal by Western blot analysis for the fourth novel PKC isoform, PKCη, in either

genotype. Given that we saw differential expression of PKCδ in control and *Nras*^{G12D} LSKs at baseline, we wanted to understand if PKCδ expression was increased following cellular stress and could therefore mitigate apoptosis in *Nras*^{G12D} HSCs. To answer this question, we collected protein lysate from control and *Nras*^{G12D} LSKs following *in vivo* radiation. Interestingly, PKCδ expression was increased in both control and *Nras*^{G12D} LSKs after radiation (Fig. 3F). Taken together, these data suggest that PKCδ is activated in primitive *Nras*^{G12D} hematopoietic cells and is further enhanced in response to radiation.

We next examined if PKCδ inhibition could, in fact, diminish the antiapoptotic effects in *Nras*^{G12D} HSCs. Both genetic and chemical inhibition of PKCδ were tested to understand this. First, we used shRNA to knockdown PKCδ in both control and *Nras*^{G12D} HSCs (Fig. 4A and B) and measured caspase activation following cytokine starvation, as described previously (Fig. 4C). Notably, knockdown of PKCδ abrogated the protective effects of N-Ras^{G12D} in HSCs, after cytokine starvation (Fig. 4C). Next, we wanted to understand the role of PKC signaling *in vivo* and irradiated (3 Gy) control and *Nras* mutant mice, and administered two intraperitoneal injections of either vehicle or PKC inhibitor AEB (Fig. 4D). Twenty-four hours after radiation, bone marrow was harvested, and cellular apoptosis measured by Annexin staining. Notably, administration of PKC inhibition *in vivo* abrogated, at least in part, the protective effects of N-Ras^{G12D} following radiation (Fig. 4E and F). Together, these data support that PKC signaling is required by N-Ras^{G12D}–induced survival of HSC/Ps under stress conditions.

N-Ras^{G12D} mitigates oxidative stress to promote survival of HSC/Ps

HSC fitness relies on the tight regulation of ROS (23, 31–35) whereas dysregulation of redox balance by γ-irradiation and chemotherapy is a well-described biochemical mechanism that induces apoptosis, specifically during Ras-mediated tumorigenesis (36–38). Thus, we asked if oncogenic N-Ras^{G12D} could alter ROS levels in HSCs and progenitors. To investigate this, we labeled freshly harvested bone marrow cells with CellRox, a fluorescent dye specific for cellular ROS, and found that *Nras*^{G12D} HSCs had reduced levels of ROS relative to control HSCs (Fig. 5A). Similar to the results of apoptosis, a reduction of ROS was not present in *Nras* mutant lineage positive cells but did remain lower in early primitive hematopoietic cells, LSKs (Fig. 5A).

Next, to determine whether levels of ROS correlate with apoptosis, we stained wild-type HSCs with both CellRox and Annexin V following *in vivo* radiation of control mice (3 Gy). As expected, HSCs with the highest ROS levels demonstrated the highest Annexin V positivity, whereas those with lower ROS were less apoptotic (Fig. 5B; Supplementary Fig. S5). We next examined ROS levels in control and *Nras*^{G12D} mice after radiation. As hypothesized, there was no difference in Annexin V positivity between control and *Nras*^{G12D} HSCs that have similar levels of ROS (Fig. 5C), whereas analysis of the wild-type and *Nras* mutant HSCs with nonoverlapping ROS levels confirmed that *Nras* mutant HSCs had lower levels of apoptosis than control HSCs (Fig. 5C). Together, these data indicate that apoptosis is diminished in *Nras*^{G12D} HSCs, at least in part, due to lower levels of ROS. To understand if HSC cell death could be attenuated through reduced ROS, sorted HSCs from control and *Nras*^{G12D} mice were treated with the anti-oxidant N-acetyl cysteine (NAC; 100

μmol/L) and subjected to 18 hours of cytokine starvation. Notably, NAC rescued wild-type HSCs from apoptosis compared with vehicle-treated HSCs but had minimal impact on *Nras*^{G12D} HSCs (Fig. 5D), indicating that HSC survival is tightly associated with redox balance under stress and N-Ras^{G12D}–induced survival of HSCs is at least partially mediated by lowering ROS levels.

Given that redox levels are intimately coupled to cell proliferation and the metabolic demands of a cell, we used previously generated *Col1A1-H2B-GFP; Rosa26-M2-rtTA* (H2B-GFP) mice (17) to study survival and levels of ROS in quiescent and cycling HSCs. In these mice, HSCs can be labeled with H2B-GFP during a 6-week period of doxycycline administration and HSC proliferation can be followed during a subsequent 12- to 18-week chase period without doxycycline. We previously reported that all SLAM HSCs are GFP^{+} after 6 weeks of doxycycline treatment (16). After an 18-week chase period, however, HSCs can be characterized as proliferative (GFP^{low}, about 80% of total HSCs) or quiescent HSCs (GFP^{high}, about 20% of total HSCs) and therefore readily separated by FACS (Supplementary Fig. S1). To understand if cell proliferation contributed to the survival benefit induced by N-Ras^{G12D}, quiescent (GFP^{high}) and cycling (GFP^{low}) HSCs from control and *Nras*^{G12D} mice were sorted and subjected to cytokine starvation for 18 hours. Although our previous data showed that N-Ras^{G12D} promotes proliferation of cycling (GFP^{low}) HSCs but reduces proliferation of quiescent (GFP^{high}) HSCs (16), both quiescent and cycling *Nras*^{G12D} HSC fractions were more resistant to apoptosis under conditions of cytokine starvation (Fig. 5E), indicating that the survival advantage is a fundamental effect of N-Ras signaling, rather than a consequence of changes in cell cycle. Furthermore, *Nras*^{G12D} HSCs had lower levels of ROS levels in both GFP^{high} and GFP^{low} fractions, suggesting that N-Ras^{G12D} reduces ROS irrespective of proliferative status (Fig. 5F and G). As expected, GFP^{low} HSCs from both genotypes had higher levels of ROS than GFP^{high} HSCs, consistent with a more proliferative and metabolically active cell population (Fig. 5F and G).

To determine the mechanism by which N-Ras^{G12D} reduces ROS in HSCs, we considered processes that could either enhance ROS detoxification or decrease ROS production. First, we measured the levels of total and oxidized glutathione and did not detect any difference between the *Nras* mutant and control LSKs (Supplementary Fig. S6A). In addition, gene expression by microarray analysis did not reveal differences in the levels of the master antioxidant regulator, NRF2, and its targets genes, or genes with known function in HSC maintenance and redox regulation, including *foxo3* and *bmi1* (Supplementary Fig. S6B). To confirm these findings, we measured mRNA levels of the NRF2 target, *Hmox1, Nqo1*, and *Gclm* by qRT-PCR and did not see any significant differences between control and *Nras*^{G12D} HSCs (Supplementary Fig. S6C). Taken together, enhanced antioxidant signaling is unlikely the mechanism by which N-Ras^{G12D} reduces ROS in HSCs. Next, we determined if ROS production is decreased in *Nras*^{G12D} HSCs. The majority of ROS is derived from bioenergetic processes in the mitochondria (39, 40), and we thus questioned if N-Ras^{G12D} induced changes in mitochondrial metabolism in HSCs. To examine metabolic activity, we measured commonly used metabolic output parameters including mitochondrial membrane potential (via TMRM staining) and ATP (via CellTiter-Glo). We found that *Nras*^{G12D} HSCs demonstrated overall lower mitochondrial membrane potential and ATP levels (Fig. 6A

and B). Notably, this phenotype was again limited to HSCs and early progenitors and not seen in total bone marrow or lineage-committed cells (Fig. 6A; Supplementary Fig. S7A). Of note, we found no significant differences in mitochondrial DNA content as measured by the ratio of mitochondrial DNA to nuclear DNA by qPCR, between control and *Nras*^{G12D} LSKs (Fig. 6C), suggesting N-Ras^{G12D} dysregulates mitochondrial metabolic activity rather than mitochondrial biogenesis. To validate this phenotype, we used a second mouse model, *Vav1-Cre*$^{+}$*; Nras*$^{LSL\text{-}G12D/+}$, which allows activation of *Nras*^{G12D} within the hematopoietic compartment during embryogenesis and does not require activation by pIpC injection (41). Consistently, HSCs from *Vav1-cre*$^{+}$*; Nras*$^{LSL\text{-}G12D/+}$ mice showed lower levels of ROS and mitochondrial membrane potential and no differences in mitochondrial DNA content compared with wild-type control littermates (Supplementary Fig. S7B–S7D). Again, this phenotype was limited to HSCs and early progenitors and not observed in lineage-committed cells (Supplementary Fig. S7B and S7C). Taken together, these data suggest that oncogenic N-Ras^{G12D} diminishes oxidative stress specifically in the HSC and early progenitor compartments, at least in part, by remodeling metabolism.

Given the role of PKC signaling in apoptosis and cellular metabolism, we next determined if PKC mediates survival of *Nras* mutant HSCs by modulating ROS metabolism. A recent report identified PKCδ as an important modulator of HSCs, which directly linked metabolic activity with HSC function and survival (42). We observed that PKC inhibition at least partially blocked the survival of *Nras* mutant HSCs (Fig. 4E and F). We next determined if PKC inhibition would raise levels of ROS in HSCs. First, we exposed 3,000 FACS-sorted wild-type CD48^{-}LSKs to PKC inhibitor, AEB, and cultured for 12 hours. Following this incubation, we observed significantly higher levels of ROS (Fig. 6D) in the AEB-treated group. To test the effect of PKC inhibition on ROS levels *in vivo*, we sublethally irradiated (3 Gy) control and *Nras*^{G12D} mice and then administered two doses of AEB via intraperitoneal injection at 12 and 18 hours after radiation (Fig. 4D). We found that *in vivo* treatment with AEB significantly decreased PKCδ protein level (Fig. 3F), and abrogated N-Ras^{G12D}–mediated reductions in ROS (Fig. 6E and F). Together with the findings that PKC inhibition abolished N-Ras^{G12D}–induced survival benefit after stress, these data support the hypothesis that N-Ras^{G12D} utilizes PKC signaling, specifically via activation of PKCδ, to mitigate oxidative stress and promote survival in HSCs and that this effect may be mediated, at least in part, through reprogrammed metabolism.

Discussion

The pathologic role of oncogenic *RAS* mutations has been well-established across a spectrum of solid tumors through elegant work in pancreatic, lung, and colon cancers. In hematologic malignancies, although mutations in *RAS* and Ras-activating genes are frequently detected (2), the pathologic role of oncogenic Ras mutations, particularly in adult leukemia, are still being debated. As sequencing sensitivity improves and data from larger clinical studies become available, mutations in *RAS* and Ras pathways are being identified as frequent molecular lesions in pediatric cancers and are enriched when evaluating high-risk, refractory and relapsed cancers across a spectrum of disease subtypes. These studies include pediatric embryonal rhabdomyosarcoma (43), neuroblastoma (4, 44), AML (3), and relapsed acute lymphoblastic leukemia, myelodysplastic syndrome, and neuroblastoma

(4, 5, 45, 46). In addition, mutations in *RAS* and Ras-activating genes in hematologic malignancies are associated with treatment resistance across a range of therapies, including IDH, FLT3, and JAK inhibitors and steroids (3, 7, 9, 47). Here, we show that oncogenic Ras signaling supports HSC/P survival through reduced ROS after exposure to metabolic or genotoxic stress, therefore providing mechanistic evidence of how oncogenic Ras maintains transformed HSC/P pools after treatment that promotes disease relapse.

Uncontrolled tumor growth requires massive cell and substrate turnover and, thus, many cancers have altered metabolism and dysregulated levels of ROS (48). Previous studies have linked the activation of several oncogenes, including *RAS, BCR-ABL*, and *FLT3-ITD*, with increased levels of ROS during malignant transformation (49–51). In contrast, during early tumorigenesis, oncogenic K-Ras was shown to induce the redox regulator, NRF2, thus lowering ROS and enhancing early pancreatic tumor formation (52). We show that, analogous to this effect, endogenously expressed oncogenic N-Ras confers a similar “redox low” phenotype in HSCs, although likely through a different mechanism. $Nras^{G12D}$ HSCs display similar levels of redox gene expression (Supplementary Fig. S6B and S6C) and comparable levels of total and oxidized glutathione (Supplementary Fig. S6A), but rather exhibit lower mitochondrial activity (Fig. 6A–C). This subsequently leads to a reduction of ROS and ultimately confers a survival benefit (Fig. 5). These results are in line with other studies describing how cancer “stem-like” populations drive treatment resistance via redox programs (36, 53, 54). Unique to HSCs, however, is that dissipation of redox stress may also provide a functional advantage, as oxidative stress is intimately linked to their differentiation, proliferation, and, ultimately, depletion (32, 55–58). Our data also show that the reduced ROS (Fig. 5A) and metabolic phenotype (Fig. 6A–C; Supplementary Fig. S7A–S7D) was limited to the HSC and early progenitor compartment and not lineage-committed cells. Thus, defining the altered biochemical dependencies and pathways in transformed HSC/Ps may provide fundamental insights into both normal and malignant hematopoiesis and highlights how studying these primitive cells may identify discrete targets distinct from the leukemic bulk.

Once activated, Ras proteins trigger extensive downstream signaling cascades that often promote uncontrolled cell proliferation (1) and, illustratively, tumor growth. Despite extensive clinical efforts to target oncogenic Ras signaling through MEK, AKT, and mTOR pathways, the efficacy of inhibiting these pathways is often modest and short-lived, suggesting a refractory population persists throughout treatment. Here, we show that the biochemical effects of oncogenic Ras signaling within the HSC/P compartment confer a survival advantage (Figs. 1 and 2) and therefore may form the basis of relapse. Importantly, these effects are not mediated by the canonical Ras effector pathways, but depends on a noncanonical Ras effector, PKCδ (Figs. 3 and 4). Although there are likely isoform, tissue and context-specific effects of PKC signaling and apoptosis, PKCδ has been identified to regulate HSC maintenance and metabolism (42). Our studies here indicate that PKCδ is activated by oncogenic N-Ras and mediates the prosurvival phenotype and metabolic remodeling of *Nras* mutant HSCs. Interestingly, although the study from Rao and colleagues (42) showed that PKCδ knockout increased ROS and mitochondrial activity likely through increased mitochondrial mass, our results here revealed that PKC activation in $Nras^{G12D}$ HSCs led to increased ROS and mitochondrial activity without affecting mitochondrial

mass. Therefore, the mechanism through which PKC regulates mitochondria function seems to be complex and context dependent. Finally, PKCδ has been shown to promote tumorigenesis in oncogenic K-Ras–mediated lung cancer and additional isoforms have been associated with inferior survival in lung and breast cancers (59, 60). Furthermore, inhibition of PKC has been reported to mitigate growth of lymphoma (61) and pancreatic cancer (62), and has been identified as one of the kinases targeted by dasatinib (63) and midostaurin (64). Combined, these studies highlight how PKC may contribute to tumorigenesis and serve as a therapeutic target, and thus, warrants further investigation.

Supplementary Material

Refer to Web version on PubMed Central for supplementary material.

Acknowledgments

The authors thank the University of Michigan Flow Cytometry Shared Resource Laboratory (supported by the NCI of the NIH under award number P30CA046592) and the University of Michigan Unit for Laboratory Animal Medicine for technical assistance and mouse colony maintenance, respectively. They also thank R. Coolon for genotyping and mouse colony management. This work was supported by NIH/NHLBI T32 (5-T32-HL007622), NIH K12 (5-K12-HD028820-25), Hyundai Hope on Wheels Young Investigator Award, and a St. Baldrick's Fellow Award with Tough Like Ike Support (to G.M. Ney), and NIH/NHLBI R01HL132392 and 1R01HL150707, American Cancer Society (125080-RSG-13-253-01-LIB), American Society of Hematology, the V Foundation for Cancer Research, Gabrielle's Angel Foundation, and University of Michigan Rogel Cancer Center research grants (to Q. Li).

References

1. Simanshu DK, Nissley DV, McCormick F. RAS proteins and their regulators in human disease. Cell 2017;170:17–33. [PubMed: 28666118]
2. Ward AF, Braun BS, Shannon KM. Targeting oncogenic Ras signaling in hematologic malignancies. Blood 2012;120:3397–406. [PubMed: 22898602]
3. Amatangelo MD, Quek L, Shih A, Stein EM, Roshal M, David MD, et al. Enasidenib induces acute myeloid leukemia cell differentiation to promote clinical response. Blood 2017;130:732–41. [PubMed: 28588019]
4. Eleveld TF, Oldridge DA, Bernard V, Koster J, Colmet Daage L, Diskin SJ, et al. Relapsed neuroblastomas show frequent RAS-MAPK pathway mutations. Nat Genet 2015;47:864–71. [PubMed: 26121087]
5. Irving J, Matheson E, Minto L, Blair H, Case M, Halsey C, et al. Ras pathway mutations are prevalent in relapsed childhood acute lymphoblastic leukemia and confer sensitivity to MEK inhibition. Blood 2014;124:3420–30. [PubMed: 25253770]
6. Jerchel IS, Hoogkamer AQ, Aries IM, Steeghs EMP, Boer JM, Besselink NJM, et al. RAS pathway mutations as a predictive biomarker for treatment adaptation in pediatric B-cell precursor acute lymphoblastic leukemia. Leukemia 2018;32:931–40. [PubMed: 28972594]
7. McMahon CM, Ferng T, Canaani J, Wang ES, Morrissette JJD, Eastburn DJ, et al. Clonal selection with RAS pathway activation mediates secondary clinical resistance to selective FLT3 inhibition in acute myeloid leukemia. Cancer Discov 2019;9:1050–63. [PubMed: 31088841]
8. Santos FPS, Getta B, Masarova L, Famulare C, Schulman J, Datoguia TS, et al. Prognostic impact of RAS-pathway mutations in patients with myelofibrosis. Leukemia 2020;34:799–810. [PubMed: 31628430]
9. Winter PS, Sarosiek KA, Lin KH, Meggendorfer M, Schnittger S, Letai A, et al. RAS signaling promotes resistance to JAK inhibitors by suppressing BAD-mediated apoptosis. Sci Signal 2014;7:ra122. [PubMed: 25538080]

10. Rossi DJ, Jamieson CH, Weissman IL. Stems cells and the pathways to aging and cancer. Cell 2008;132:681–96. [PubMed: 18295583]
11. Saito Y, Kitamura H, Hijikata A, Tomizawa-Murasawa M, Tanaka S, Takagi S, et al. Identification of therapeutic targets for quiescent, chemotherapy-resistant human leukemia stem cells. Sci Transl Med 2010;2:17ra9.
12. Shlush LI, Zandi S, Mitchell A, Chen WC, Brandwein JM, Gupta V, et al. Identification of pre-leukaemic haematopoietic stem cells in acute leukaemia. Nature 2014;506:328–33. [PubMed: 24522528]
13. Corces-Zimmerman MR, Hong WJ, Weissman IL, Medeiros BC, Majeti R. Preleukemic mutations in human acute myeloid leukemia affect epigenetic regulators and persist in remission. Proc Natl Acad Sci U S A 2014;111: 2548–53. [PubMed: 24550281]
14. Li Q, Haigis KM, McDaniel A, Harding-Theobald E, Kogan SC, Akagi K, et al. Hematopoiesis and leukemogenesis in mice expressing oncogenic NrasG12D from the endogenous locus. Blood 2011;117:2022–32. [PubMed: 21163920]
15. Wang J, Liu Y, Li Z, Wang Z, Tan LX, Ryu MJ, et al. Endogenous oncogenic Nras mutation initiates hematopoietic malignancies in a dose- and cell type-dependent manner. Blood 2011;118:368–79. [PubMed: 21586752]
16. Li Q, Bohin N, Wen T, Ng V, Magee J, Chen SC, et al. Oncogenic Nras has bimodal effects on stem cells that sustainably increase competitiveness. Nature 2013;504:143–7. [PubMed: 24284627]
17. Foudi A, Hochedlinger K, Van Buren D, Schindler JW, Jaenisch R, Carey V, et al. Analysis of histone 2B-GFP retention reveals slowly cycling hematopoietic stem cells. Nat Biotechnol 2009;27:84–90. [PubMed: 19060879]
18. Domen J The role of apoptosis in regulating hematopoietic stem cell numbers. Apoptosis 2001;6:239–52. [PubMed: 11445666]
19. Kiel MJ, Yilmaz OH, Iwashita T, Yilmaz OH, Terhorst C, Morrison SJ. SLAM family receptors distinguish hematopoietic stem and progenitor cells and reveal endothelial niches for stem cells. Cell 2005;121:1109–21. [PubMed: 15989959]
20. Mohrin M, Bourke E, Alexander D, Warr MR, Barry-Holson K, Le Beau MM, et al. Hematopoietic stem cell quiescence promotes error-prone DNA repair and mutagenesis. Cell Stem Cell 2010;7:174–85. [PubMed: 20619762]
21. Warr MR, Binnewies M, Flach J, Reynaud D, Garg T, Malhotra R, et al. FOXO3A directs a protective autophagy program in haematopoietic stem cells. Nature 2013;494:323–7. [PubMed: 23389440]
22. Williams GT, Smith CA, Spooncer E, Dexter TM, Taylor DR. Haemopoietic colony stimulating factors promote cell survival by suppressing apoptosis. Nature 1990;343:76–9. [PubMed: 1688645]
23. Ho TT, Warr MR, Adelman ER, Lansinger OM, Flach J, Verovskaya EV, et al. Autophagy maintains the metabolism and function of young and old stem cells. Nature 2017;543:205–10. [PubMed: 28241143]
24. Mortensen M, Soilleux EJ, Djordjevic G, Tripp R, Lutteropp M, Sadighi-Akha E, et al. The autophagy protein Atg7 is essential for hematopoietic stem cell maintenance. J Exp Med 2011;208:455–67. [PubMed: 21339326]
25. Sumitomo Y, Koya J, Nakazaki K, Kataoka K, Tsuruta-Kishino T, Morita K, et al. Cytoprotective autophagy maintains leukemia-initiating cells in murine myeloid leukemia. Blood 2016;128:1614–24. [PubMed: 27480114]
26. Garcia-Prat L, Martinez-Vicente M, Perdiguero E, Ortet L, Rodríguez-Ubreva J, Rebollo E, et al. Autophagy maintains stemness by preventing senescence. Nature 2016;529:37–42. [PubMed: 26738589]
27. Whelan RD, Parker PJ. Loss of protein kinase C function induces an apoptotic response. Oncogene 1998;16:1939–44. [PubMed: 9591777]
28. Mochly-Rosen D, Das K, Grimes KV. Protein kinase C, an elusive therapeutic target? Nat Rev Drug Discov 2012;11:937–57. [PubMed: 23197040]

29. Zhuang S, Demirs JT, Kochevar IE. Protein kinase C inhibits singlet oxygen-induced apoptosis by decreasing caspase-8 activation. Oncogene 2001;20: 6764–76. [PubMed: 11709711]
30. Steinberg SF. Structural basis of protein kinase C isoform function. Physiol Rev 2008;88:1341–78. [PubMed: 18923184]
31. Ito K, Hirao A, Arai F, Takubo K, Matsuoka S, Miyamoto K, et al. Reactive oxygen species act through p38 MAPK to limit the lifespan of hematopoietic stem cells. Nat Med 2006;12:446–51. [PubMed: 16565722]
32. Mantel CR, O'Leary HA, Chitteti BR, Huang X, Cooper S, Hangoc G, et al. Enhancing hematopoietic stem cell transplantation efficacy by mitigating oxygen shock. Cell 2015;161:1553–65. [PubMed: 26073944]
33. Miyamoto K, Araki KY, Naka K, Arai F, Takubo K, Yamazaki S, et al. Foxo3a is essential for maintenance of the hematopoietic stem cell pool. Cell Stem Cell 2007;1:101–12. [PubMed: 18371339]
34. Tothova Z, Kollipara R, Huntly BJ, Lee BH, Castrillon DH, Cullen DE, et al. FoxOs are critical mediators of hematopoietic stem cell resistance to physiologic oxidative stress. Cell 2007;128:325–39. [PubMed: 17254970]
35. Yahata T, Takanashi T, Muguruma Y, Ibrahim AA, Matsuzawa H, Uno T, et al. Accumulation of oxidative DNA damage restricts the self-renewal capacity of human hematopoietic stem cells. Blood 2011;118:2941–50. [PubMed: 21734240]
36. Diehn M, Cho RW, Lobo NA, Kalisky T, Dorie MJ, Kulp AN, et al. Association of reactive oxygen species levels and radioresistance in cancer stem cells. Nature 2009;458:780–3. [PubMed: 19194462]
37. Lagadinou ED, Sach A, Callahan K, Rossi RM, Neering SJ, Minhajuddin M, et al. BCL-2 inhibition targets oxidative phosphorylation and selectively eradicates quiescent human leukemia stem cells. Cell Stem Cell 2013; 12:329–41. [PubMed: 23333149]
38. Shaw AT, Winslow MM, Magendantz M, Ouyang C, Dowdle J, Subramanian A, et al. Selective killing of K-ras mutant cancer cells by small molecule inducers of oxidative stress. Proc Natl Acad Sci U S A 2011;108:8773–8. [PubMed: 21555567]
39. Balaban RS, Nemoto S, Finkel T. Mitochondria, oxidants, and aging. Cell 2005; 120:483–95. [PubMed: 15734681]
40. Adam-Vizi V, Chinopoulos C. Bioenergetics and the formation of mitochondrial reactive oxygen species. Trends Pharmacol Sci 2006;27:639–45. [PubMed: 17056127]
41. Georgiades P, Ogilvy S, Duval H, Licence DR, Charnock-Jones DS, Smith SK, et al. VavCre transgenic mice: a tool for mutagenesis in hematopoietic and endothelial lineages. Genesis 2002;34:251–6. [PubMed: 12434335]
42. Rao TN, Gupta MK, Softic S, Wang LD, Jang YC, Thomou T, et al. Attenuation of PKCdelta enhances metabolic activity and promotes expansion of blood progenitors. EMBO J 2018;37:e100409. [PubMed: 30446598]
43. Itzykson R, Kosmider O, Renneville A, Morabito M, Preudhomme C, Berthon C, et al. Clonal architecture of chronic myelomonocytic leukemias. Blood 2013;121: 2186–98. [PubMed: 23319568]
44. Ackermann S, Cartolano M, Hero B, Welte A, Kahlert Y, Roderwieser A, et al. A mechanistic classification of clinical phenotypes in neuroblastoma. Science 2018; 362:1165–70. [PubMed: 30523111]
45. Lindsley RC, Saber W, Mar BG, Redd R, Wang T, Haagenson MD, et al. Prognostic mutations in myelodysplastic syndrome after stem-cell transplantation. N Engl J Med 2017;376:536–47. [PubMed: 28177873]
46. Oshima K, Khiabanian H, da Silva-Almeida AC, Tzoneva G, Abate F, Ambesi-Impiombato A, et al. Mutational landscape, clonal evolution patterns, and role of RAS mutations in relapsed acute lymphoblastic leukemia. Proc Natl Acad Sci U S A 2016;113:11306–11. [PubMed: 27655895]
47. Aries IM, van den Dungen RE, Koudijs MJ, Cuppen E, Voest E, Molenaar JJ, et al. Towards personalized therapy in pediatric acute lymphoblastic leukemia: RAS mutations and prednisolone resistance. Haematologica 2015;100:e132–6. [PubMed: 25480501]

48. Vander Heiden MG, DeBerardinis RJ. Understanding the intersections between metabolism and cancer biology. Cell 2017;168:657–69. [PubMed: 28187287]

49. Irani K, Xia Y, Zweier JL, Sollott SJ, Der CJ, Fearon ER, et al. Mitogenic signaling mediated by oxidants in Ras-transformed fibroblasts. Science 1997; 275:1649–52. [PubMed: 9054359]

50. Sattler M, Verma S, Shrikhande G, Byrne CH, Pride YB, Winkler T, et al. The BCR/ABL tyrosine kinase induces production of reactive oxygen species in hematopoietic cells. J Biol Chem 2000;275:24273–8. [PubMed: 10833515]

51. Sallmyr A, Fan J, Datta K, Kim KT, Grosu D, Shapiro P, et al. Internal tandem duplication of FLT3 (FLT3/ITD) induces increased ROS production, DNA damage, and misrepair: implications for poor prognosis in AML. Blood 2008; 111:3173–82. [PubMed: 18192505]

52. DeNicola GM, Karreth FA, Humpton TJ, Gopinathan A, Wei C, Frese K, et al. Oncogene-induced Nrf2 transcription promotes ROS detoxification and tumorigenesis. Nature 2011;475:106–9. [PubMed: 21734707]

53. Agathocleous M, Meacham CE, Burgess RJ, Piskounova E, Zhao Z, Crane GM, et al. Ascorbate regulates haematopoietic stem cell function and leukaemogenesis. Nature 2017;549:476–81. [PubMed: 28825709]

54. Cimmino L, Dolgalev I, Wang Y, Yoshimi A, Martin GH, Wang J, et al. Restoration of TET2 function blocks aberrant self-renewal and leukemia progression. Cell 2017;170:1079–95. [PubMed: 28823558]

55. Owusu-Ansah E, Banerjee U. Reactive oxygen species prime Drosophila haematopoietic progenitors for differentiation. Nature 2009;461:537–41. [PubMed: 19727075]

56. Park IK, Qian D, Kiel M, Becker MW, Pihalja M, Weissman IL, et al. Bmi-1 is required for maintenance of adult self-renewing haematopoietic stem cells. Nature 2003;423:302–5. [PubMed: 12714971]

57. Yu WM, Liu X, Shen J, Jovanovic O, Pohl EE, Gerson SL, et al. Metabolic regulation by the mitochondrial phosphatase PTPMT1 is required for hematopoietic stem cell differentiation. Cell Stem Cell 2013;12:62–74. [PubMed: 23290137]

58. Vannini N, Girotra M, Naveiras O, Nikitin G, Campos V, Giger S, et al. Specification of haematopoietic stem cell fate via modulation of mitochondrial activity. Nat Commun 2016;7:13125. [PubMed: 27731316]

59. Symonds JM, Ohm AM, Carter CJ, Heasley LE, Boyle TA, Franklin WA, et al. Protein kinase C delta is a downstream effector of oncogenic K-ras in lung tumors. Cancer Res 2011;71:2087–97. [PubMed: 21335545]

60. Zurgil U, Ben-Ari A, Rotem-Dai N, Karp G, Krasnitsky E, Frost SA, et al. PKCeta is an anti-apoptotic kinase that predicts poor prognosis in breast and lung cancer. Biochem Soc Trans 2014;42:1519–23. [PubMed: 25399563]

61. Chang G, Zheng J, Xiao W, Chang S, Wei Q, Wu H, et al. PKC inhibition of sotrastaurin has antitumor activity in diffuse large B-cell lymphoma via regulating the expression of MCT-1. Acta Biochim Biophys Sin 2018;50: 399–407. [PubMed: 29534146]

62. Cheng J, Tian L, Ma J, Gong Y, Zhang Z, Chen Z, et al. Dying tumor cells stimulate proliferation of living tumor cells via caspase-dependent protein kinase Cdelta activation in pancreatic ductal adenocarcinoma. Mol Oncol 2015;9:105–14. [PubMed: 25156550]

63. Tobio A, Alfonso A, Botana LM. C-kit mutations determine dasatinib mechanism of action in HMC-1 neoplastic mast cells: dasatinib differently regulates PKCdelta translocation in HMC-1(560) and HMC-1(560,816) cell lines. Immunopharmacol Immunotoxicol 2015;37:380–7. [PubMed: 26181649]

64. Stone RM, Manley PW, Larson RA, Capdeville R. Midostaurin: its odyssey from discovery to approval for treating acute myeloid leukemia and advanced systemic mastocytosis. Blood Adv 2018;2:444–53. [PubMed: 29487059]

Significance:

Targeting oncogenic N-Ras–mediated reduction of ROS in hematopoietic stem cells through inhibition of the noncanonical Ras effector PKC may serve as a novel strategy for treatment of leukemia and other Ras-mutated cancers.

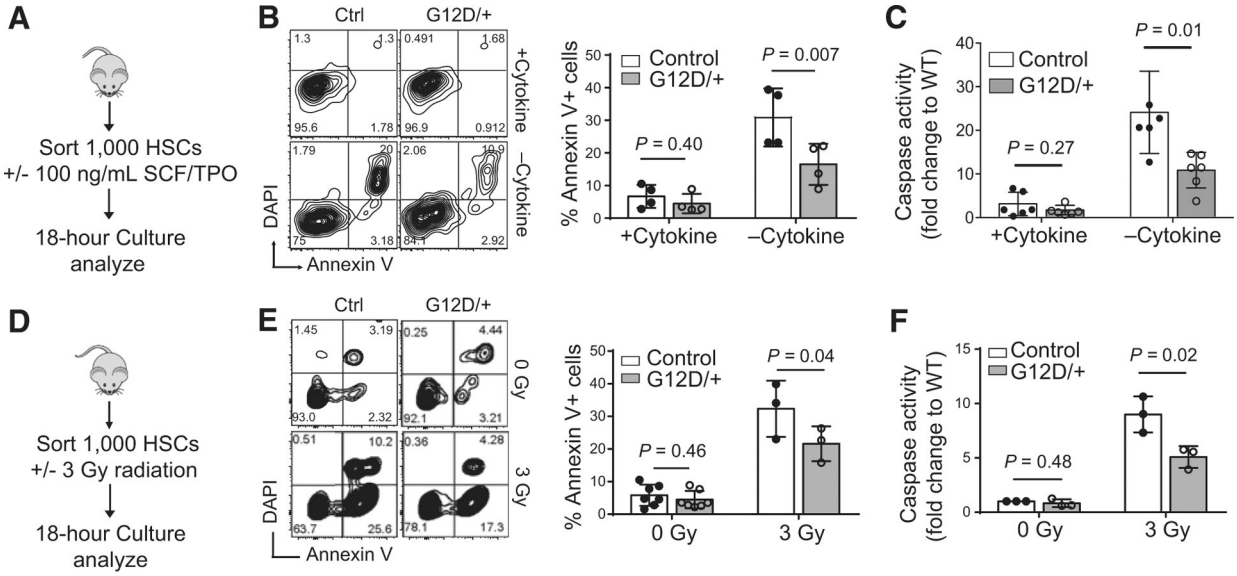

Figure 1.

N-Ras$^{G12D/+}$ confers HSC survival to exogenous stress *in vitro*. **A,** Experimental design for in vitro cytokine starvation. **B,** Representative flow cytometry plot for Annexin V and DAPI staining with quantitative representation ($n = 4$). Paired Student t test was used to calculate statistical significance. **C,** Survival, as measured by caspase activation, of control or Nras^{G12D} SLAM HSCs cultured in cytokine-rich (SCF+TPO; 100 ng/mL) or starved SF-03 media ($n = 6$). Two-tailed unpaired Student t test was used to calculate statistical significance. WT, wild-type. **D,** Experimental design for *in vitro* radiation. **E,** Representative flow cytometry plot for Annexin V and DAPI staining following radiation with quantitative representation ($n = 7$ for 0 Gy, $n = 3$ for 3 Gy). Paired Student t test was used to calculate statistical significance. **F,** Survival of FACS-sorted control or *Nras*^{G12D} HSCs, as measured by caspase activation, after exposure to 300 cGy of *in vitro* γ-radiation ($n = 3$). Two-tailed unpaired Student t test was used to calculate statistical significance. Data represent mean ± SD; n, number of mice.

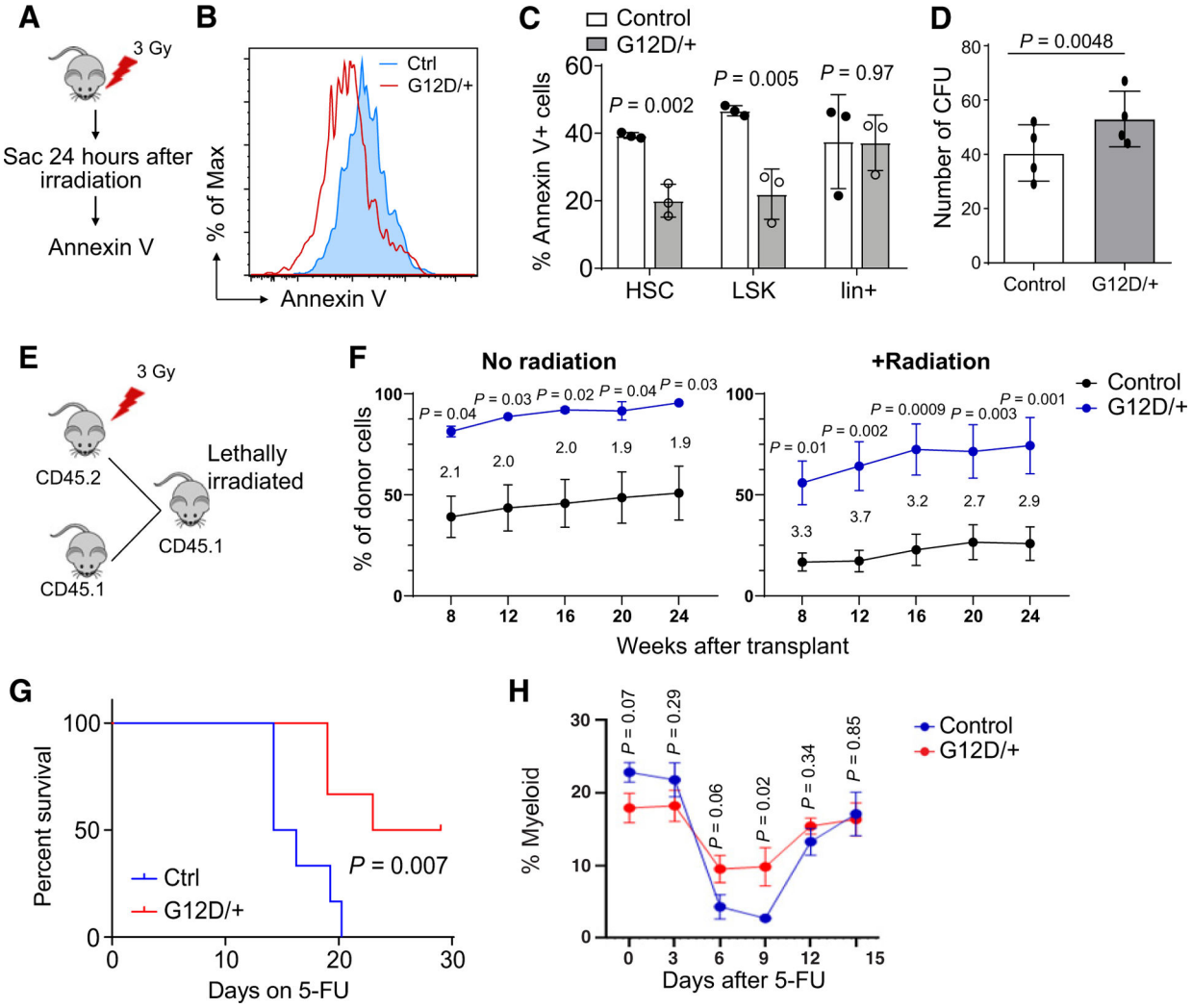

Figure 2.

N-Ras^{G12D} protects HSCs and early progenitors from apoptosis following *in vivo* γ-radiation **A,** Experimental scheme showing exposure of control and *Nras* mutant mice to 300 cGy of γ-radiation *in vivo*. **B,** Representative flow cytometry histogram of Annexin V staining in control and *Nras* mutant mice 24 hours following *in vivo* radiation. **C,** Bone marrow from control and *Nras* mutant mice harvested and stained for Annexin using SLAM HSC markers (HSC: Lineage^{-}c-kit^{+}Sca-1^{+}CD48^{-}CD150^{+}; LSK: Lineage^{-}c-kit^{+}Sca-1^{+}; Lin^{+}: all but Lineage^{-}; $n = 3$). Two-tailed Student *t* test was used to calculate statistical significance. **D,** A total of 400 SLAM HSCs were FACS sorted and plated into duplicate wells containing murine Methocult media (M3434; Stem Cell Technologies) 24 hours following *in vivo* radiation (300 cGy) of control and *Nras* mutant mice. Colonies counted at day 7 of culture ($n = 4$). Paired *t* test was used for statistical analysis. CFU, colony-forming units. **E,** Experimental design to radiate *Nras* mutant and control mice prior to competitive transplant. **F,** Donor cell contribution to CD45^{+} cells in transplant recipients of *Nras* mutant or control donors. Wild-type competitor CD45.1 cells were mixed at a 1:1 ratio with unirradiated donor cells and at 1:10 ratio for irradiated donors (two donors were

used for total of five to eight recipients). Unpaired *t* test was used to calculate statistical significance. Fold change for each time point is shown between the curves. **G,** Survival curve of control and $Nras^{G12D}$ mice following weekly 5-FU injections (150 mg/kg/dose; $n = 6$). Log-rank test was used for statistical analysis. **H,** The percentage of myeloid cells in peripheral blood following a single dose of 5-FU ($n = 7$). Two-tailed Student *t* test was used to calculate statistical significance. Data represent mean ± SD; *n*, number of mice.

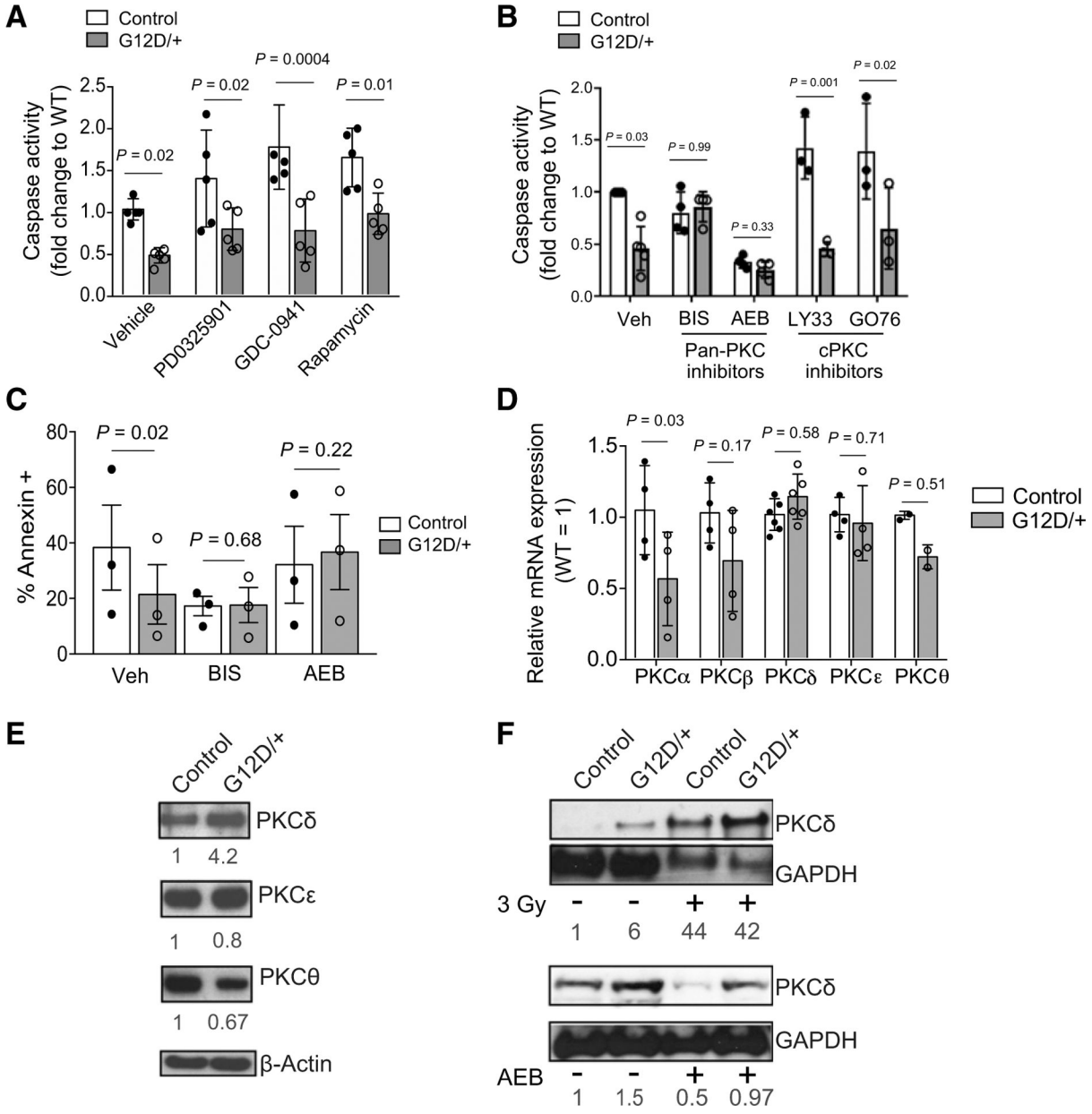

Figure 3.

N-Ras^{G12D}–induced prosurvival phenotype of HSCs is dependent on noncanonical Ras effector PKC signaling. **A,** SLAM HSCs from control and *Nras* mutant mice were FACS sorted into SF-03 media under conditions of cytokine starvation in the presence of either vehicle control, MEK inhibitor (PD0325901; 100 nmol/L), PI3K inhibitor (GDC-0941; 399 nmol/L), or mTOR inhibitor (rapamycin; 100 nmol/L), and apoptosis was measured by caspase activation following 18 hours of culture (n = 4–6). Two-way ANOVA was used for statistical significance. WT, wild-type. **B,** SLAM HSCs from control and *Nras* mutant mice were FACS sorted into SF-03 media under conditions of cytokine starvation in the presence of either vehicle control (Veh), pan-PKC inhibitors (BIS 5 μmol/L; AEB 10 μmol/L), or inhibitors to classic PKCs (LY33 1 μmol/L; GO76 10 μmol/L). Following 18 hours of

culture, apoptosis was measured by caspase activation (n = 3–5). Two-way ANOVA was used for statistical significance. **C,** SLAM HSCs from control and *Nras* mutant mice were FACS sorted into SF-03 media under conditions of cytokine starvation in the presence of either vehicle control or pan-PKC inhibitors (BIS 5 μmol/L; AEB 10 μmol/L). Following 18 hours of culture, apoptosis was measured by Annexin V staining (n = 3). Paired t test was used for statistical significance. **D,** mRNA levels, as measured by qRT-PCR, of PKC isoforms in SLAM HSCs isolated from control or *Nras* mutant mice (n = 2–6). Unpaired Student t test was used to calculate statistical significance. **E,** Western blots on 20,000 LSKs from control and *Nras* mutant mice showing the expression of novel PKC isoforms: PKCδ, PKCε, PKCθ. β-actin was used as a loading control (n = 3). Relative expression (as signal ratio of PKC isoform to β-actin) was quantified from three independent blots and is shown below each blot. **F,** Western blots showing the expression of PKCδ prior to and following *in vivo* radiation (top; LSKs) or following *in vivo* treatment with the PKC inhibitor AEB (bottom; cKit-enriched cells). GAPDH level was used as a loading control. Relative expression (as signal ratio of PKCδ to GAPDH) was quantified from three independent blots and is shown. Data represent mean ± SD; n, number of mice.

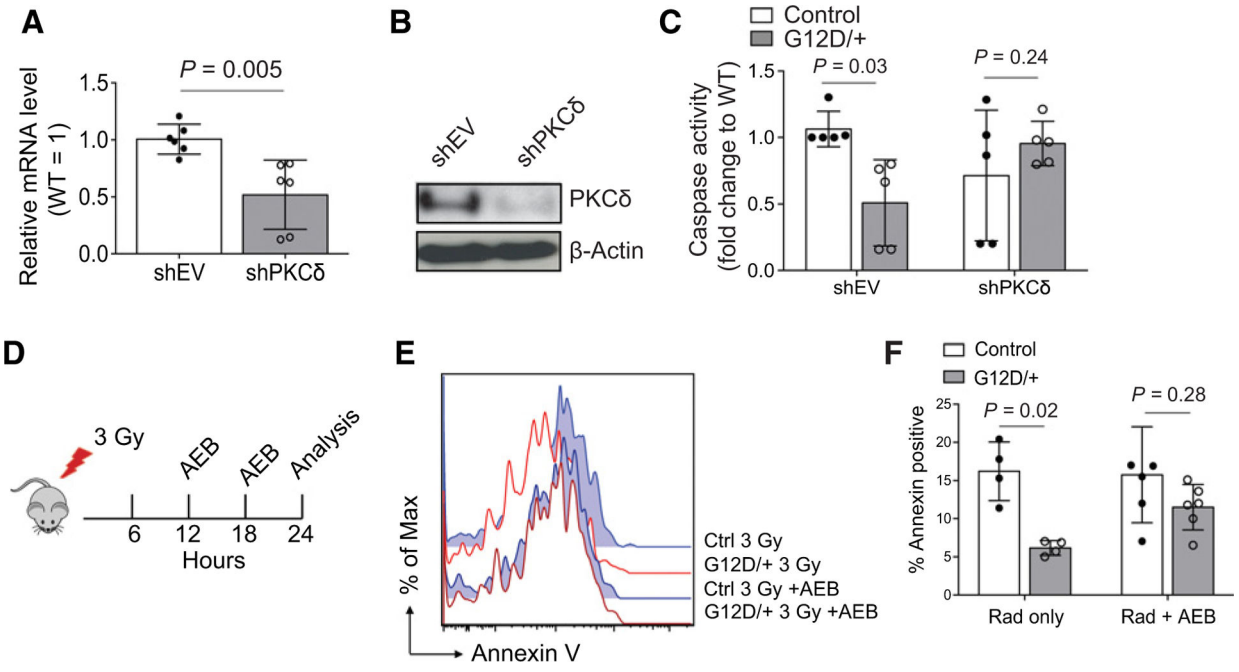

Figure 4.

Inhibition of PKC ameliorates prosurvival benefit conferred to HSCs by N-Ras^{G12D}. **A** and **B,** c-kit–enriched cells were transfected with either empty vector control or PKCδ shRNA, and mRNA level by qRT-PCR (**A**) and protein level by Western blot analysis (**B**) was measured to verify knockdown ($n = 6$). Unpaired Student t test was used to calculate statistical significance. WT, wild-type. **C,** FACS-purified SLAM HSCs from control or *Nras* mutant mice were exposed to cytokine starvation following transfection with either empty vector or PKCδ shRNA, and apoptosis was measured after 18 hours of culture using caspase activation ($n = 5$). Two-way ANOVA was used for statistical significance. **D,** Experimental design using *in vivo* administration of the PKC inhibitor AEB (10 μg/g body mass) to sensitize HSCs to apoptosis with and without γ-radiation. **E** and **F,** Representative flow cytometry histogram (**E**) and quantitation (**F**) showing apoptosis of SLAM HSCs as measured by Annexin V staining following *in vivo* radiation alone or together with AEB treatment in control and *Nras* mutant mice ($n = 4–6$). Two-way ANOVA was used for statistical significance. Data represent 10 mean ± SD; *n*, number of mice.

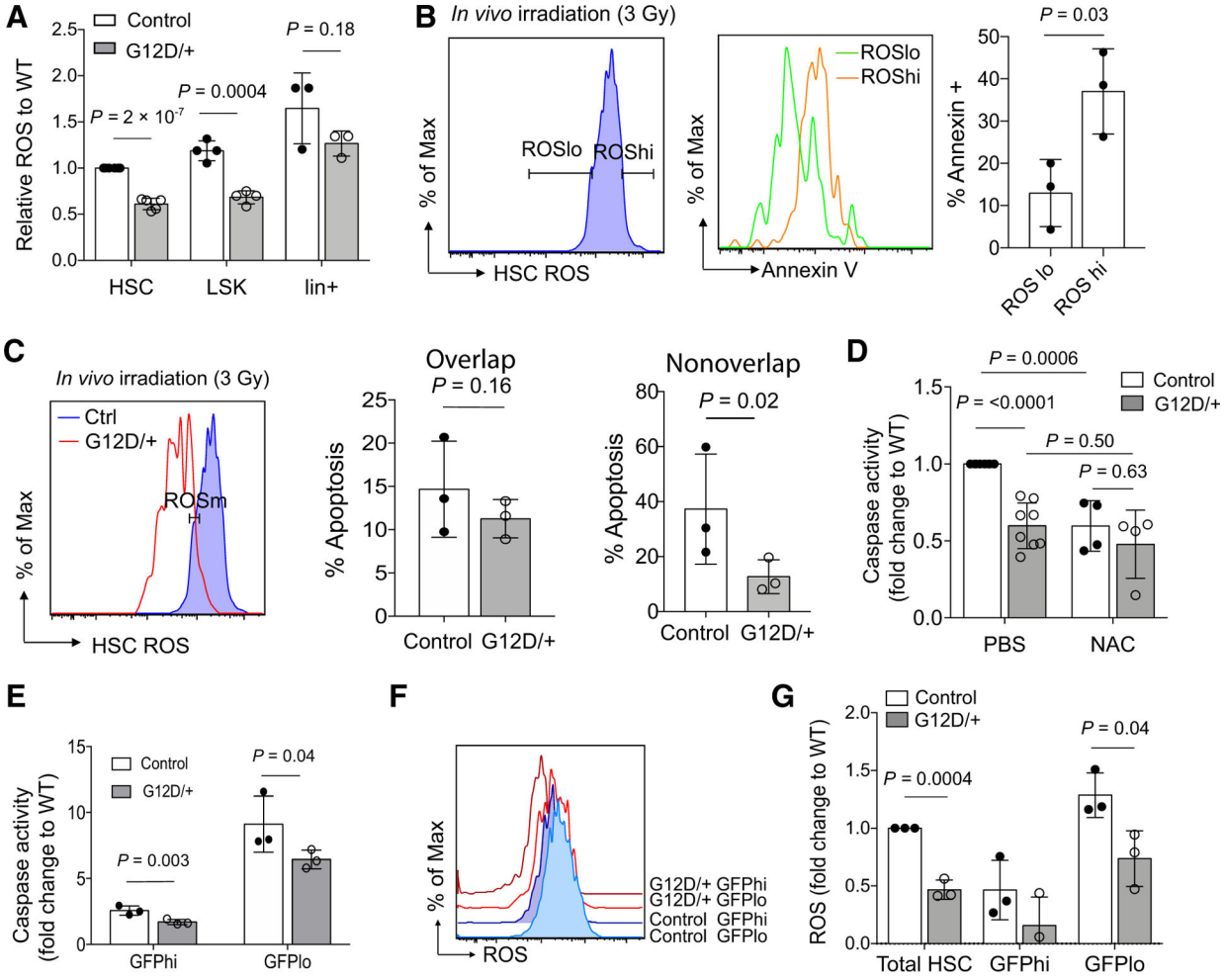

Figure 5.

N-Ras^{G12D} lowers ROS in HSCs and early progenitors and affords a prosurvival advantage to HSCs. **A,** Levels of cellular ROS measured by CellRox in HSC, LSK, and lineage-positive hematopoietic compartments in control and *Nras* mutant mice ($n = 4$). Student *t* test was used to determine statistical significance. WT, wild-type. **B,** Levels of apoptosis, as measured by Annexin V staining, in ROS^{lo} (lowest 10% of HSCs) and ROS^{hi} (highest 10% of HSCs) populations in wild-type mice following *in vivo* radiation ($n = 3$). Student *t* test was used to determine statistical significance. **C,** Levels of apoptosis, as measured by Annexin V staining, in wild-type and *Nras* mutant HSC with overlapping (left) or nonoverlapping (right) ROS levels (measured by CellRox staining) following *in vivo* radiation ($n = 3$). Paired Student *t* test was used to determine statistical significance. **D,** FACS-purified HSCs from control or *Nras* mutant mice were exposed to cytokine starvation for 18 hours in the presence or absence of N-acetyl cysteine (100 μmol/L), and apoptosis was measured by caspase activation ($n = 4$). Two-way ANOVA was used to determine statistical significance. **E**–**G**, Control and *Nras*^{G12D} mice that carry *Col1A1-H2B-GFP; Rosa26-M2-rtTA* (H2B-GFP) transgenes were treated with doxycycline for 6 weeks, followed by a 16-week no doxycycline chase period. SLAM HSCs were then FACS sorted into GFP^{hi} and GFP^{lo} populations (Supplementary Fig. S1). Apoptosis (**E**) was measured

by caspase activation following cytokine starvation (18 hours) *in vitro* ($n = 3$). ROS levels (**F** and **G**) were measured by CellRox ($n = 3$). Paired Student *t* test was used to determine statistical significance. Of note, no *P* value was calculated for GFP^{hi} cells in **G** because of a negative value in the $Nras^{G12D}$ group. Data represent mean ± SD; *n*, number of mice.

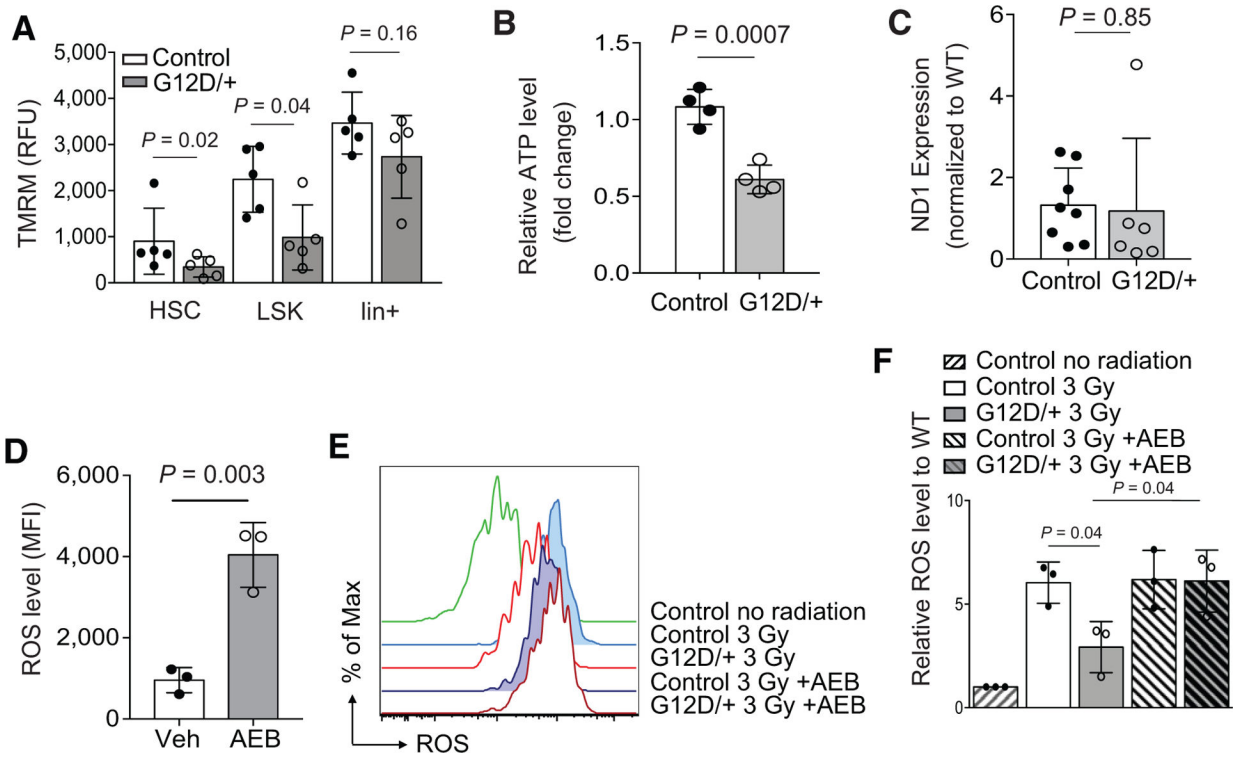

Figure 6.

N-Ras^{G12D} reduces mitochondrial activity and ATP contents in HSCs. **A,** Mitochondrial membrane potential as measured by TMRM in hematopoietic populations from control or *Nras* mutant (G12D/+) mice ($n = 5$). Paired Student t test was used to determine statistical significance. RFU, relative fluorescent units. **B,** ATP levels of HSCs (400 SLAM HSCs) from control and *Nras* mutant mice ($n = 4$). Unpaired Student t test was used to determine statistical significance. **C,** Mitochondrial content, as measured by the ratio of mitochondrial (copies of ND1 gene) to nuclear (copies of β-actin gene) DNA. DNA was extracted from FACS-sorted 40,000 control and *Nras*^{G12D} LSKs by DirectTail lysis reagent with proteinase K. ND1 (mitochondrial-encoded gene) copies were quantified by qPCR and normalized to β-actin ($n = 8$). Unpaired Student t test was used to determine statistical significance. **D,** Wild-type SLAM HSCs were treated *in vitro* with the pan-PKC inhibitor AEB, and levels of ROS were measured by flow cytometry using CellRox ($n = 3$). Unpaired Student t test was used to calculate statistical significance. MFI, mean fluorescence intensity. **E** and **F,** Control or *Nras* mutant mice were irradiated (300 cGy) and injected with two doses (6 and 12 hours after radiation) of AEB (10 μg/g body mass), and ROS levels were measured 24 hours after radiation ($n = 3$). ANOVA was used to calculate statistical significance. Data represent mean ± SD; n, number of mice.